Research Article | Vol. 24, No. 14 | 11 Jul 2016 | OPTICS EXPRESS 15872

Optics EXPRESS

Highly sensitive gas leak detector based on a quartz-enhanced photoacoustic SF6 sensor

ANGELO SAMPAOLO,[1,2] PIETRO PATIMISCO,[1,2] MARILENA GIGLIO,[1] LEONARDO CHIECO,[3] GAETANO SCAMARCIO,[1] FRANK K. TITTEL,[2] AND VINCENZO SPAGNOLO[1,2,*]

[1]*Dipartimento Interateneo di Fisica, Università e Politecnico di Bari, CNR-IFN UOS BARI, Via Amendola 173, Bari, Italy*
[2]*Department of Electrical and Computer Engineering, Rice University, 6100 Main Street, Houston, TX 77005, USA*
[3]*MASMEC S.p.A., Via dei Gigli, 21, Modugno BA, Italy*
[*]*vincenzoluigi.spagnolo@poliba.it*

Abstract: The implementation, performance validation, and testing of a gas-leak optical sensor based on mid-IR quartz-enhanced photoacoustic (QEPAS) spectroscopic technique is reported. A QEPAS sensor was integrated in a vacuum-sealed test station for mechatronic components. The laser source for the sensor is a quantum cascade laser emitting at 10.56 μm, resonant with a strong absorption band of sulfur hexafluoride (SF_6), which was selected as a leak tracer. The minimum detectable concentration of the QEPAS sensor is 2.7 parts per billion with an integration time of 1 s, corresponding to a sensitivity of leak flows in the 10^{-9} mbar·l/s range, comparable with state-of-the-art leak detection techniques.

OCIS codes: (280.3420) Laser sensors; (140.5965) Semiconductor lasers, quantum cascade; (300.6390) Spectroscopy, molecular.

References and links

1. S. T. Moe, K. Schjølberg-Henriksen, D. T. Wang, E. Lund, J. Nysæther, L. Furuberg, M. Visser, T. Fallet, and R. W. Bernstein, "Capacitive differential pressure sensor for harsh environments," Sensor. Actuat. A-Phys. **83**, 30–33 (2000).
2. L. G. Harus, M. Cai, K. Kawashima, and K. Toshiharu, "Determination of temperature recovery time in differential-pressure-based air leak detector," Meas. Sci. Technol. **17**(2), 411–418 (2006).
3. P. E. Mix, *Leak Testing Methods, in Introduction to Nondestructive Testing: A Training Guide* (John Wiley & Sons, Inc., 2004).
4. S. Millar and M. Desmulliez, "MEMS ultra low leak detection methods: a review," Sens. Rev. **29**(4), 339–344 (2009).
5. S. Kai-lei and S. Xin-li, "Summary of the theory and method of vacuum helium-mass-spectroscopy leak detection," Vacuum Electronics **6**, 62–65 (2007).
6. A. Calcatelli, M. Bergoglio, and D. Mari, "Leak detection, calibrations and reference flows: practical example," Vacuum **81**(11-12), 1538–1544 (2007).
7. N. Javahiraly, "Review on hydrogen leak detection: comparison between fiber optic sensors based on different designs with palladium," Opt. Eng. **54**(3), 030901 (2015).
8. I. Galli, S. Bartalini, S. Borri, P. Cancio, D. Mazzotti, P. De Natale, and G. Giusfredi, "Molecular gas sensing below parts per trillion: radiocarbon-dioxide optical detection," Phys. Rev. Lett. **107**(27), 270802 (2011).
9. Q. Tan, X. Pei, S. Zhu, D. Sun, J. Liu, C. Xue, T. Liang, W. Zhang, and J. Xiong, "Development of an optical gas leak sensor for detecting ethylene, dimethyl ether and methane," Sensors (Basel) **13**(4), 4157–4169 (2013).
10. A. Elia, P. M. Lugarà, C. Di Franco, and V. Spagnolo, "Photoacoustic techniques for trace gas sensing based on semiconductor laser sources," Sensors (Basel) **9**(12), 9616–9628 (2009).
11. C. M. Lee, K. V. Bychkov, V. A. Kapitanov, A. I. Karapuzikov, Y. N. Ponomarev, I. V. Sherstov, and V. A. Vasiliev, "High-sensitivity laser photoacoustic leak detector," Opt. Eng. **46**(6), 064302 (2007).
12. P. Patimisco, G. Scamarcio, F. K. Tittel, and V. Spagnolo, "Quartz-enhanced photoacoustic spectroscopy: a review," Sensors (Basel) **14**(4), 6165–6206 (2014).
13. V. Spagnolo, P. Patimisco, S. Borri, G. Scamarcio, B. E. Bernacki, and J. Kriesel, "Part-per-trillion level SF_6 detection using a quartz enhanced photoacoustic spectroscopy-based sensor with single-mode fiber-coupled quantum cascade laser excitation," Opt. Lett. **37**(21), 4461–4463 (2012).
14. V. Spagnolo, P. Patimisco, S. Borri, G. Scamarcio, B. E. Bernacki, and J. Kriesel, "Mid-infrared fiber-coupled QCL-QEPAS sensor," Appl. Phys. B **112**(1), 25–33 (2013).

#267202 http://dx.doi.org/10.1364/OE.24.015872
Journal © 2016 Received 27 May 2016; revised 30 Jun 2016; accepted 30 Jun 2016; published 5 Jul 2016

Optics EXPRESS

15. A. Sampaolo, P. Patimisco, M. Giglio, M. S. Vitiello, H. E. Beere, D. A. Ritchie, G. Scamarcio, F. K. Tittel, and V. Spagnolo, "Improved tuning fork for terahertz quartz-enhanced photoacoustic spectroscopy," Sensors (Basel) **16**(4), 439 (2016).
16. M. Maiss and C. A. M. Brenninkmeijer, "Atmospherics SF6: trends, sources and prospects," Environ. Sci. Technol. **32**(20), 3077–3086 (1998).
17. A. A. Kosterev, F. K. Tittel, D. Serebryakov, A. Malinovsky, and A. Morozov, "Applications of quartz tuning fork in spectroscopic gas sensing," Rev. Sci. Instrum. **76**(4), 043105 (2005).
18. P. Patimisco, A. Sampaolo, M. Giglio, J. M. Kriesel, F. K. Tittel, and V. Spagnolo, "Hollow core waveguide as mid-infrared laser modal beam filter," J. Appl. Phys. **118**(11), 113102 (2015).
19. A. Sampaolo, P. Patimisco, J. M. Kriesel, F. K. Tittel, G. Scamarcio, and V. Spagnolo, "Single mode operation with mid-IR hollow fibers in the range 5.1-10.5 μm," Opt. Express **23**(1), 195–204 (2015).
20. H. R. Carlon, "Infrared absorption coefficients (3-15 μ) for sulfur hexafluoride (SF(6)) and Freon ($CCI_{(2)}F_{(2)}$)," Appl. Opt. **18**(10), 1474–1475 (1979).
21. D. M. Cox, and A. Gnauk, "Continuous wave CO_2 laser spectroscopy of SF_6, WF_6 and UF_6," J. Mol. Spectrosc. **81**, 205–215 (1980).
22. Available online: http://www.hitran.com
23. M. Giglio, P. Patimisco, A. Sampaolo, G. Scamarcio, F. K. Tittel, and V. Spagnolo, "Allan deviation plot as a tool for quartz enhanced photoacoustic sensors noise analysis," IEEE Trans. Ultrason. Ferroelectr. Freq. Control **63**(4), 555–560 (2016).
24. A. Roth, *Vacuum Technology* (Elsevier Science Publishers, 1990).
25. J. F. O'Hanlon, *A Users Guide to Vacuum Technology* (John Wiley and Sons, 1989).
26. J. M. Lafferty, *Foundations of Vacuum Science and Technology* (John Wiley and Sons, 1998).
27. A. Pregelj, M. Drab, and M. Mozetic, "Leak detection methods and defining the sizes of leaks," in *4th International Conference of Slovenian Society for Nondestructive Testing* (1997).

1. Introduction

Leak detection and localization are critical manufacturing quality-control processes for several industrial fields such as mechatronics, biotechnology, petrochemical and automotive industries. There is a need for products and technologies that require hermetically closed areas, vessels, and tubes conveying pressurized gases or liquids, where leaks are a serious threat to products reliability and safety. Consequentially, considerable effort was invested during the last decades in developing gas leak-detection systems with high sensitivity and stability to guarantee proper operation of a device in vacuum-sealed or high-pressure conditions. The selection of the leak sensing method is mainly related to the required measurement precision. Differential pressure detectors are typically employed in industrial production chains, when the measurement time period allowed is a few seconds, and the precision for a single measurement is 1 Pa. These detectors monitor the pressure difference between two environments that are isolated from each other by forcing high-pressure gas into one of them. The disadvantage of this approach is the low sensitivity and the fluctuations of repeated measurements within ~4 Pa [1, 2]. Differential-pressure test detection limits of $1x10^{-3}$ mbar·l/s can be realized.

A different category of techniques is based on the detection of specific gas species (such as inert gases). An overpressure of a mixture containing the tracer gas is made inside the element under test and leaks are detected by tracing the target gas presence in the surrounding area. Halogen leak sensors require the pressurization of the system to be tested with an organic halide. The leak is found with a sniffer probe sensitive to traces of the halogen-bearing gas. With such a system, leaks in the 10^{-7} mbar·l/s range can be identified [3]. Radioisotopes based systems are able to detect leaks as small as 10^{-10} mbar·l/s. The item to be tested is placed in a chamber, which is filled with a radioactive tracer gas (typically krypton 85) [4]. If there is a leak, the radioactive gas diffuses through it inside the item. After removing the component from the test chamber, the radioactive gas flows outside through the leaks and can be detected by a radiation sensor. Mass spectroscopy leak sensors employ helium as the gas target [5, 6]. These systems have proven to be extremely sensitive, reaching a leak flow detection range of 10^{-11} mbar·l/s, which is suitable for quality control of critical components such as, for example, vehicle airbags or cardiac pacemaker cases. Hydrogen gas can also be used. The advantage of hydrogen is its very low natural background concentration in air (0.5 part per million (ppm)). The main disadvantage is its flammability. To reduce such a risk, gas mixtures containing < 5% of H_2 in nitrogen (N_2) are employed [7].

Optics EXPRESS

In leak measurements, besides sensitivity and selectivity, the response time is important for the real-time detection of changes in gas tracer concentration. Techniques based on optical absorption for trace gas detection are fast (with response times of 1 s or less), suffer from minimal drifts, offer high gas specificity, are capable of sub-parts per trillion (ppt) concentration detection sensitivity [8] and permit real time *in situ* measurements [9]. The best results have been obtained when laser absorption techniques operate in the mid-IR fingerprint region, where most gases show their strongest absorption bands. A robust and sensitive optical detection technique is photo-acoustic spectroscopy (PAS) employing a compact and relatively low-cost detection module [10, 11]. Among the different PAS methods, quartz-enhanced photoacoustic spectroscopy (QEPAS) was demonstrated to be the most sensitive technique, reaching detection limit in the few tens of ppt range [12–14] and normalized noise-equivalent absorption values down to 10^{-11} $cm^{-1}W/Hz^{½}$ [15].

In this manuscript, the implementation of an optical leak sensor based on QEPAS is reported. The QEPAS sensor was integrated into a vacuum-seal test station for mechanical valves. Sulfur hexafluoride (SF_6) was selected as the leak tracer gas and a 1% SF_6 in N_2 mixture was employed. SF_6 is an extremely stable gas with unique physical and chemical properties that make it an ideal candidate for leak detection applications [16]. Test and validation of the leak detector system with valves and certified leaks demonstrated the feasibility to reach minimum detectable leak flow down to 10^{-9} mbar·l/s range.

2. Methodology and QEPAS sensor calibration

QEPAS is typically used for environmental monitoring of air pollution and the analysis of multicomponent gas mixtures produced in technological processes [12, 17]. In QEPAS, a quartz tuning fork (QTF) is used as the resonant electro-acoustic transducer to detect weak photoacoustic excitations, generated by the gas target absorption from an exciting laser beam. The merits of QEPAS include high detection sensitivity, high selectivity, and a fast time response and thus this technique is an excellent choice for leak detection purposes. Furthermore, QEPAS is immune to external sound sources and does not require the use of optical detectors [12].

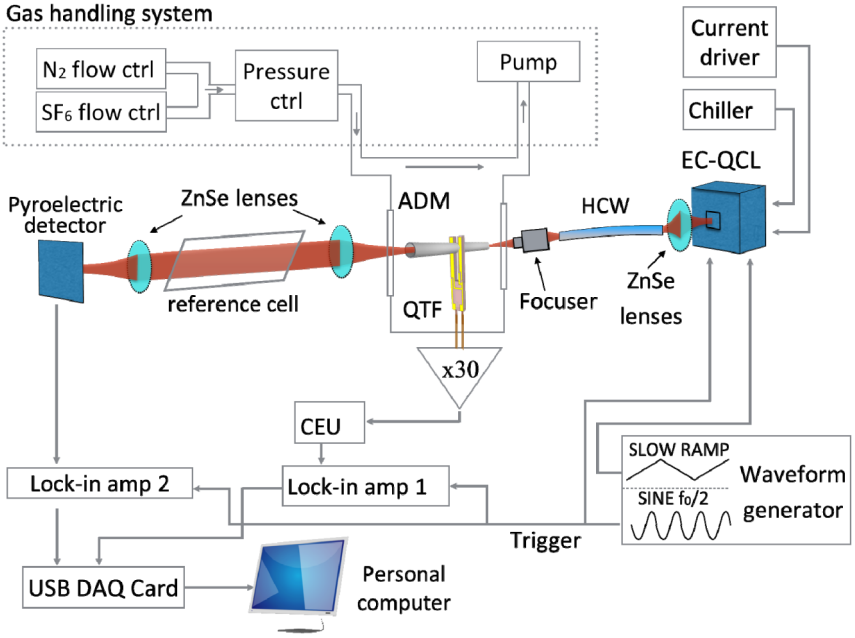

Fig. 1. Block diagram of the experimental apparatus. ADM = Acoustic detection module; QTF = Quartz tuning fork; HCW = Hollow core waveguide; EC-QCL = external cavity quantum cascade laser; CEU = Control electronics unit; DAQ = Data acquisition.

Optics EXPRESS

The typical experimental apparatus used for QEPAS detection of SF_6 is shown in Fig. 1 and is similar to that used in [13, 14]. The light source is an external-cavity quantum cascade laser (QCL) emitting at ~10.56 μm. The radiation is focused into a hollow core waveguide (HCW) with an internal diameter of 300 μm by using a ZnSe lens (focal length f = 40 mm and diameter of 1 inch). The light exiting the HCW is focused into an Acoustic Detection Module (ADM) by a focusing system [14]. The ADM contains a standard 32 kHz-QTF, two micro-resonator tubes for acoustic amplification, two ZnSe windows, and is connected to the input gas line. The ADM volume is ~2 cm^3. The use of a HCW improves the QCL beam profile by filtering out higher order modes and providing a single-mode Gaussian-like laser beam output, allowing an optimal focalization of the laser beam through the two micro resonator tubes and between the QTF prongs [18, 19]. The interaction between the radiation and the SF_6 molecules generate sound waves, which excite the vibration of the QTF prongs. The light exiting from the ADM is re-collimated using another ZnSe lens (f = 40 mm, diameter of 1 inch) and passes through a reference cell, filled with a 0.1% mixture of SF_6 in N_2.

A pyroelectric detector measures the light absorption and provides a useful spectral reference for the identification of the SF_6 absorption lines. This part of the experimental setup serves only for the QEPAS sensor calibration and validation, and was removed in the final leak test station in order to achieve sensor system compactness.

The mechanical vibrations of the QTF create a voltage signal via the piezoelectric effect. This signal is amplified by a factor 30 by means of a transimpedance amplifier (with a 10 MΩ feedback resistor) and then processed by a Control Electronics Unit (CEU). The CEU determined the main QTF parameters: resistance R, quality factor Q, and resonant frequency f_0. The CEU is also used to transfer the signal coming from the transimpedance amplifier to the lock-in amplifier. A wavelength modulation (WM) technique was implemented by applying a sinusoidal modulation to the laser current at half of the QTF resonance frequency ($f_0/2$) and detecting the QTF response at f_0 by means of a lock-in amplifier (lock-in amp 1 in Fig. 1). WM QEPAS spectral scans were performed by slowly varying the laser wavelength using a piezoelectric amplifier (not shown in Fig. 1). The output signal from the lock-in amplifier is digitalized by a National Instruments DAQ card (USB 6008), connected to a personal computer. The temporal evolution of both the piezoelectric signal and the response of the pyroelectric detector are obtained by means of LabVIEW based software. A trace gas standard generator is used to produce SF_6 concentrations in the range 0–10 ppm, using pure or humidified N_2 as the diluting gas, starting from a certified 10 ppm SF_6 in N_2 mixture. The pressure and flow rate of the gas mixture are controlled using a pressure controller (MKS Instruments Type 640) and two flow controllers (Brooks Instruments 5850S). The flow of the gas mixture was set at a constant rate of 0.67 mbar·l/s (0.67 scc/sec = 40 scc/min).

To demonstrate the use of QEPAS for leak detection, SF_6 was selected as the trace gas marker. SF_6 has its strongest absorption band in the 10.5-10.6 μm (943-952 cm^{-1}) spectral region [20,21]. In a previous work [14], we reported a simulated absorption spectrum for a gas mixture of standard air and 10 ppm of SF_6 at 75 Torr pressure in the range 947-950 cm^{-1}, using HITRAN database [22]. For the sensor operation, we selected the strongest line centered at 947.93 cm^{-1} with absorption strength of $1.4 \cdot 10^{-20}$ cm/mol, which is well separated from the only feature potentially interfering in this range: a H_2O absorption band centered at 948.26 cm^{-1}.. The laser power was set at 25 mW. The time constant of the lock-in amplifier 1 was set at 100 ms and a signal integration-time of 300 ms was selected using the LabVIEW-based acquisition program. The optimum operating condition in terms of gas pressure *P* and laser modulation voltage were identified. The conditions providing the highest signal-to-noise ratio are: gas pressure *P* = 75 Torr and peak-to-peak laser amplitude modulation voltage of 4.2 V. At these operating conditions, we performed a series of QEPAS spectral scans by varying the SF_6 concentration in the gas mixture. The QEPAS signal was measured at different SF_6 concentration levels, ranging between 132 parts per billion (ppb) and 10 ppm. Figure 2(a) shows a selection of QEPAS scans, and in Fig. 2(b) the measured peak signals as a function of the SF_6 concentration in the gas mixture are reported. The error bars associated

Optics EXPRESS

with the SF_6 concentration in Fig. 2(b) result from the sensitivity of the ow controllers, while the error bars on the QEPAS signal were determined by the related 1σ noise.

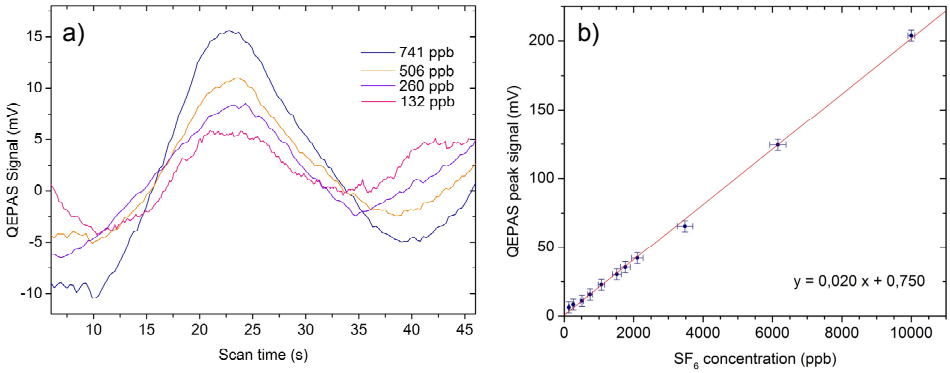

Fig. 2. a) QEPAS scans of the absorption line centered at 947.93 cm^{-1} measured for SF_6 concentrations of 741, 506, 260 and 132 ppb. The frequency of the voltage ramp used to scan the laser wavelength across the absorption line is 10 mHz. b) QEPAS peak signals as a function of the SF_6 concentration. The straight line is a linear fit of the experimental points.

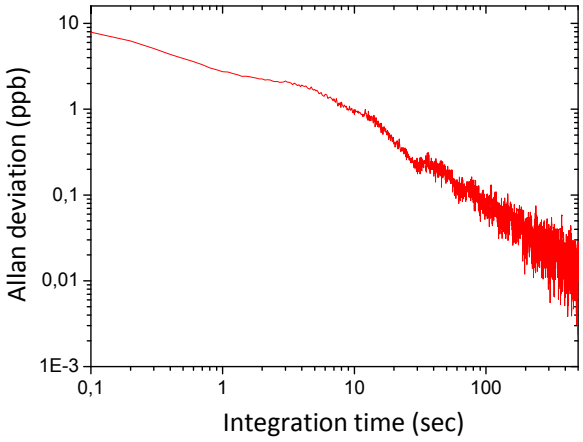

Fig. 3. Allan deviation in ppb of the QEPAS signal as a function of the integration time.

A linear fit of the experimental data points in Fig. 2(b) yields a slope of a = 0.020 mV/ppb and an intercept of b = 0.750 mV. The b value represents the resulting QEPAS background noise level. The R-squared value equals 0.999, which verifies the linearity of the QEPAS signal versus SF_6 concentration. Furthermore, we performed an Allan variance analysis to determine the achievable minimum detection limit (MDL) of the QEPAS sensor by acquiring the QEPAS signal when pure N_2 flows in the ADM for a period of 3 hours [23]. The Allan deviation plot is depicted in Fig. 3.

For an integration time of 1 s (i.e. a detection bandwidth of 0.16675 Hz), we achieved a MDL value of 2.75 ppb.

3. Leak station test and validation

A leak test station was designed and realized, by implementing the previously described QEPAS based SF_6 sensor system. This station is intended to detect and quantify leaks in mechatronics systems and components, such as vacuum-valves and diesel injectors, which must operate at high pressures. Figure 4 shows the schematic diagram of the QEPAS leak-test

Optics EXPRESS

station, which includes two pressure meters, a pressure and a flow controller as well as a certified leak inserted in a test chamber for system validation.

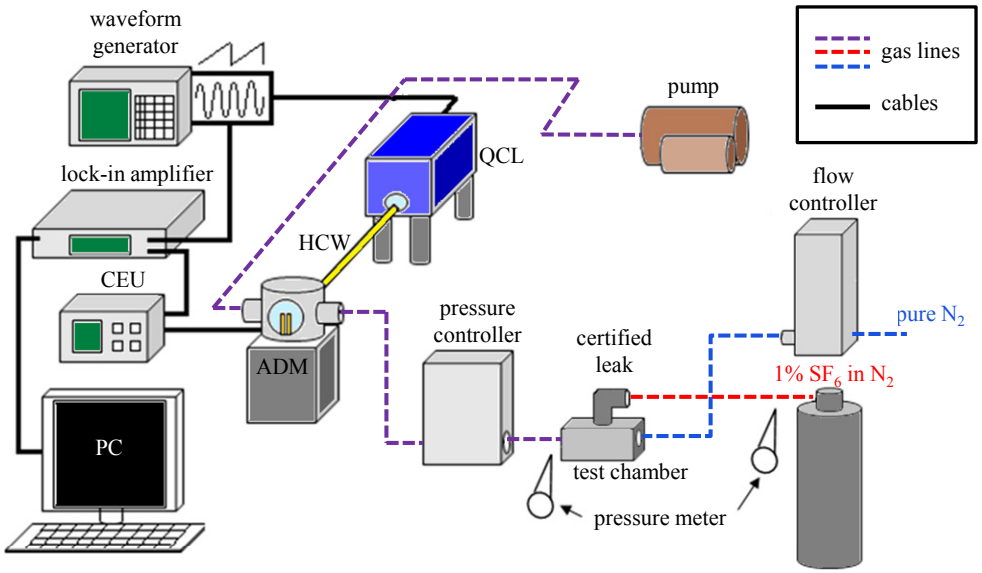

Fig. 4. Block diagram of the leak-test station. ADM = Acoustic detection module; HCW = Hollow core waveguide; QCL = quantum cascade laser; CEU = Control electronics unit; PC = Personal Computer. The dashed lines mimic the gas lines. Solid lines are electrical connections.

A calibrated leak (ATEQ, model L1147AQ-N) was used to validate the test station. A picture of this leak and the test chamber is shown in Fig. 5(a). In order to perform the validation, pure N_2 was passed through the test chamber at a level of 0.67 mbar·l/s, while an overpressure of 1% SF_6:N_2 was applied to the certified leak. A part of this mixture flows through the leak in the test chamber, due to the differential pressure (ΔP) between the test chamber and the SF_6:N_2 mixture. Thus, the gas sample coming out from the test chamber contains a SF_6 concentration, which depends on the leak size. A pressure controller allows the gas mixture to pass through the ADM at a fixed pressure of 75 Torr. In this manner, it is possible to determine the resulting SF_6 concentration using the QEPAS sensor operating in the locked mode, i.e. with the EC-QCL frequency set to the center of the selected SF_6 absorption line. The ΔP was varied between 100 mbar and 1000 mbar for validation of the QEPAS leak-test station. The resulting leak flow F_L can be calculated from the following expression:

$$F_L = \frac{F_C \cdot (S - b)}{a \cdot C_{SF_6} - (S - b)} \quad (1)$$

where F_C is the N_2 gas carrier flow (0.67 mbar·l/s), S is the QEPAS peak signal recorded for each ΔP considered, and C_{SF6} is the certified concentration of SF_6 in N_2 used as leak tracer (C_{SF6} = 0.01 in our experiments). The lock-in amplifier constant time was set at 100 ms and the extracted leak flux as a function of the selected differential pressure is reported in Fig. 5(b). The results were compared with the calibration data provided for the certified leak and a very good correlation was obtained. The discrepancies observed for differential pressures < 500 mbar are due to limitations in the differential pressure detector used for calibration when it is approaching its minimum range of leak flow detection.

Optics EXPRESS

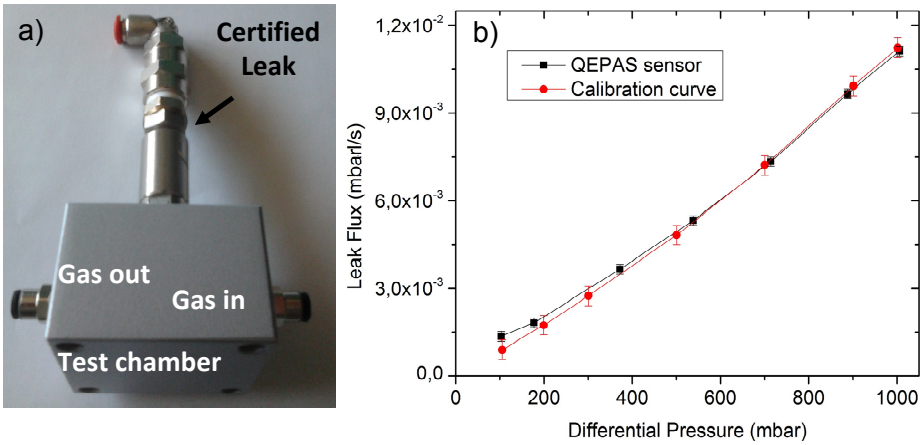

Fig. 5. a) Photo of the certified leak inserted in the test chamber. The gas-in and gas-out connectors are also visible. b) Leak flows measured as a function of differential pressure ΔP using the QEPAS sensors (■ symbols), compared with the calibration data (● symbols) provided for the certified leak.

The response time of the test station is determined by the flow rate and the length of the gas line connecting the test chamber to the ADM. Considering an ADM volume (~2 cm^3), a 20 cm-long connecting tube with a 1.6 mm internal radius, and a flow rate of 0.67 mbar·l/s, the response time of the sensor should be lower than 6 sec. However, we observed a response time of ~10 sec. This increase is due to resistance to flow introduced by tube connections and the pressure controller positioned between the test chamber and the ADM. A faster response time can be obtained by increasing the gas flow rate. Values > 1.7 mbar·l/s (100 ssc/min) should be avoided, otherwise noise components due to gas flow turbulences will occur [12].

4. Leak test station operation

Once validated, the leak test station was tested with real vacuum-valve samples. Photos of the investigated valves and of their operating principles are shown in Figs. 6(a)-6(c).

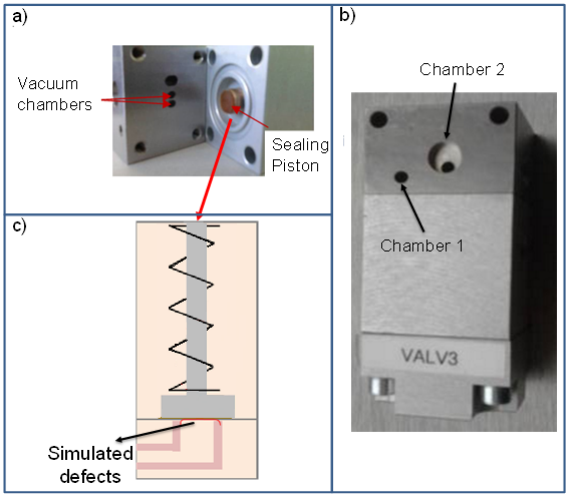

Fig. 6. a) Photo of the internal part of the investigated valves. The internal holes connected to the two valve chambers are marked by the red arrows. The sealing piston used to close the two holes is visible in the right side. b) Photo of valve 3. The entrances to the two valve chambers used to inject the test gases are marked by black arrows. c) Schematic of the valve operation principle. The sealing piston pushes over the two internal holes to isolate them. Defects of the

Optics EXPRESS

valves were simulated by inserting a small wire (small red line in the picture) between the two holes, as marked by the black arrow.

The vacuum valves contain two separated chambers with internal (see Fig. 6(a)) and external (see Fig. 6(b)) connecting holes. A sealing piston, pushed by a pressure of 5 bars, closes the two internal holes and isolates the two chambers. Pure N_2 flows into valve chamber 1 (see Fig. 6(b)), while an overpressure of 1% SF_6:N_2 is created in chamber 2 via the related external holes. In absence of any defect, the sealing piston is able to isolate the two chambers, avoiding contamination of the pure N_2 flow from SF_6 leak tracer gas. We investigated valves with and without simulated defects. These defects were realized by inserting small metallic wires between the two internal holes, as schematically depicted in Fig. 6(c). In this way, the wires allow SF_6 contamination into chamber 1. Wires of different diameters, ranging from 20 μm to 170 μm were inserted between the internal holes. Figure 7 depicts a picture and a schematic of the test station with a valve under test. The gas delivery system used to connect the two chambers with pure N_2 and the SF_6:N_2 leak gas tracer is also shown. During the valve test, a flux of 0.67 mbar·l/s of N_2 flows through chamber 1, while chamber 2 is filled with the 1% SF_6:N_2 mixture at an overpressure of 400 mbar.

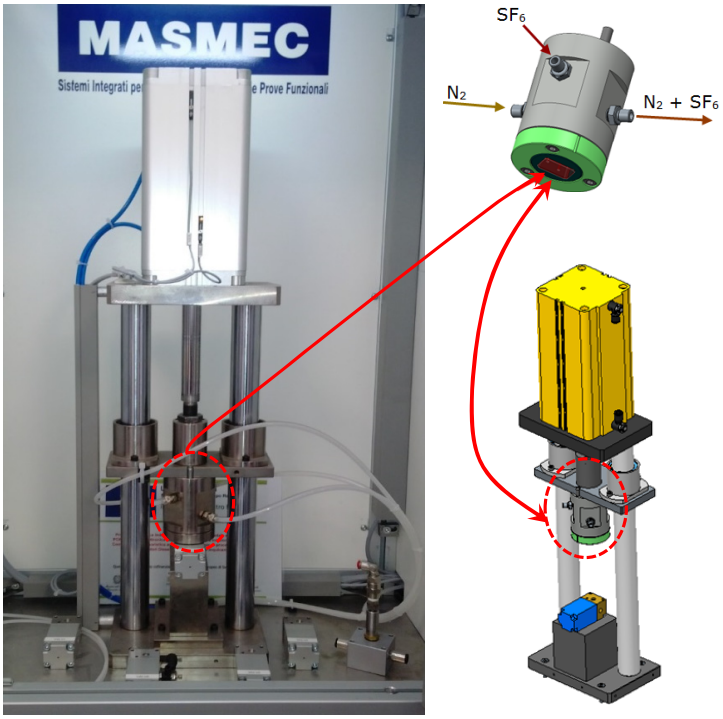

Fig. 7. Photo and schematic of the valve-seal test station and of the gas delivery system used to connect the two valve chambers. The red dashed circles mark the position of the gas delivery system in the test station.

The QEPAS sensor is operated in the scan mode. The concentration of the resulting SF_6 trace contamination is extracted using the calibration curve reported in Fig. 2(b). The spectral scans obtained for the valve without defect and four valves with defects of different size are shown in Fig. 8.

Optics EXPRESS

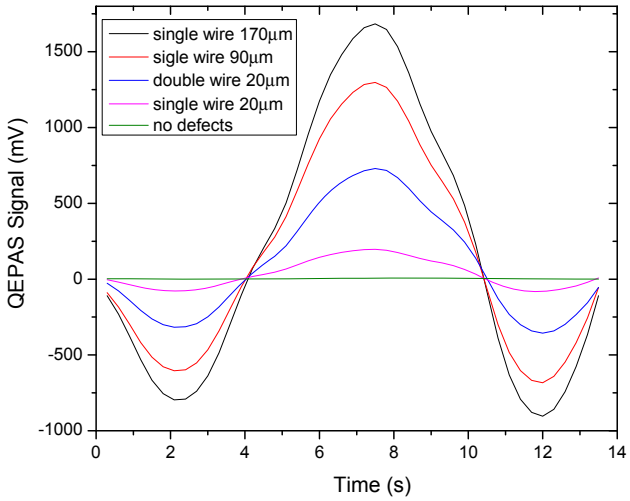

Fig. 8. QEPAS scans of the absorption line centered at 947.93 cm^{-1} measured for five different valve samples. The frequency of the voltage ramp used to scan the laser wavelength across the SF_6 absorption line is 25 mHz. The related types of defects are reported in the legend.

The leak flows for each valve were calculated using Eq. (1) starting from the corresponding QEPAS peak signal *S*. The obtained leak flow values for the five valves are listed in Table 1.

Table 1. QEPAS peak signals and related leak flows calculated using Eq. (1) for a valve without defects (*valve1*) and four valves incorporating different defects. The corresponding SF_6 contaminations (in ppm) in the N_2 flow are also reported and were extracted using the calibration curve reported in Fig. 2(b).

Valve (type of defect)	QEPAS peak Signal (mV)	Leak flows (10^{-3} mbar·l/s)	SF_6 contamination (ppm)
valve1 **(no-defects)**	1.10	$3.3 \cdot 10^{-3}$	0.02
valve2 **(20 µm wire)**	201.11	0.67	10.02
valve3 **(20 µm double-wire)**	734.69	2.45	36.70
valve4 **(90 µm wire)**	1299.66	4.36	64.94
valve5 **(170 µm wire)**	1684.86	5.66	84.21

For valve 1 (without defects), as expected, only noise level leaks were measured, while the valve with the biggest defect (*valve5*) generates a leak flow of $5.66 \cdot 10^{-3}$ mbar·l/s. This value is close to the minimum detectable leak for a differential pressure detector. The leak detected for the smallest defect was $6.7 \cdot 10^{-4}$ mbar·l/s, measured for *valve2*. However, the corresponding SF_6 trace-gas concentration (10.02 ppm) is three orders of magnitude higher than the QEPAS sensor MDL value. Starting from a QEPAS sensor noise-equivalent concentration of 2.75 ppb at 1 sec integration time and considering a N_2 gas carrier flow of 0.67 mbar·l/s, it is possible to estimate the minimum detectable leak at these conditions, using Eq. (1). This results in a leak of ~$4.5 \cdot 10^{-7}$ mbar·l/s, which can be decreased to ~$4.5 \cdot 10^{-9}$ mbar·l/s if pure SF_6 is used as leak test gas. A further decrease of the minimum detectable leak could be obtained by reducing the pure N_2 flux. However, values below ~0.17 mbar·l/s (10 scc/min) are not practical, since the time needed for the SF_6 leak trace to reach the QEPAS sensor would exceed several tens of seconds. Note that, leak-test station operations do not necessarily require QEPAS spectral scans. Leaks detection can be also performed by

Optics EXPRESS

maintaining the laser wavelength on the selected SF_6 absorption line and measuring the temporal QEPAS signal evolution.

Figure 9 depicts a comparison of the QEPAS leak detector performance obtained in this investigation with other reported gas leak-detection methods sensitivities in the literature [24–27]. Our optical leak station is competitive with state-of-the-art techniques, reaching sensitivity level obtainable only with radioisotope and mass spectroscopy systems, and with the advantages of lower cost, compact size and weight, faster response time and not requiring radioactive materials.

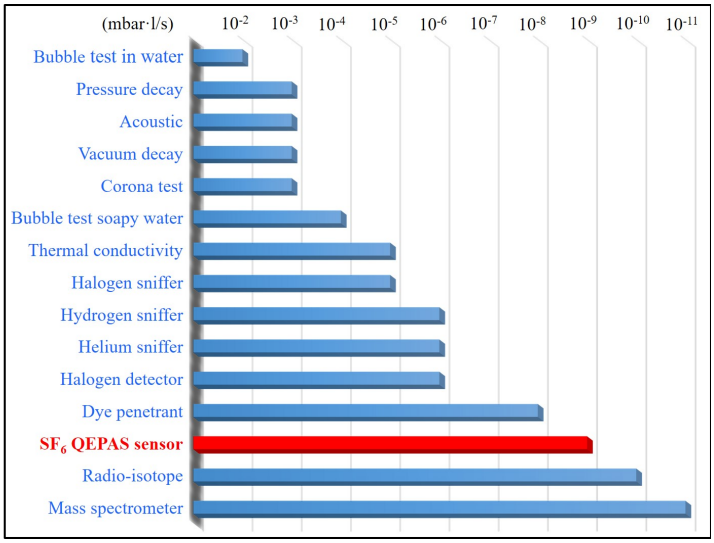

Fig. 9. Sensitivity ranges in mbar·l/s of the main leak detection methods.

5. Conclusions

A leak test station employing a QEPAS sensor was demonstrated, calibrated and its performance was validated. The SF_6 QEPAS sensor shows a minimum detection sensitivity of 2.75 ppb for a 1 s integration time, which corresponds to a minimum detectable leak for the test station of $4.5 \cdot 10^{-7}$ mbar·l/s, if a N_2 gas carrier flow of 0.67 mbar·l/s is used. The leak flow detectivity could reach $\sim 1 \cdot 10^{-9}$ mbar·l/s, if a N_2 flow of < 0.17 mbar·l/s and pure SF_6 are employed. This reported SF_6 QEPAS leak detection technique is competitive with most leak-detection systems reported in the literature, with distinct advantages, such as a much faster response time, compactness, lower weight and cost as well as safety. Finally, since the leak due to vacuum chamber defects are proportional to the tracer gas overpressure, the sensitivity of the reported test station to defects of automotive items can be further improved by increasing the pressure of the SF_6:N_2 mixture, within the mechanical limits of the items being tested .

Funding

Ministero dell'Istruzione, dell'Università e della Ricerca (PON02 00675 and PON02 00576); National Science Foundation (NSF) (ERC MIRTHE awards); USA Robert Welch Foundation (R4925S).